Check for updates

Received: 12 February 2026 | Revised: 25 March 2026 | Accepted: 23 April 2026

DOI: 10.1002/ar.70216

RESEARCH ARTICLE

The Anatomical Record | American Association for Anatomy | WILEY

Tracing the evolutionary history of the morpho-anatomy of baculum in primates

Federica Spani[1] | **Maria Pia Morigi**[2] | **Matteo Bettuzzi**[2,3] | **Monica Carosi**[3]

[1]Department of Science and Bio-Technology, Università Campus Bio-Medico di Roma, Roma, Italy

[2]Department of Physics and Astronomy "Augusto Righi", University of Bologna, Bologna, Italy

[3]Department of Sciences, University Roma Tre, Rome, Italy

Correspondence
Federica Spani, Via Alvaro del Portillo, 21, 00128 Roma, Italy.
Email: f.spani@unicampus.it

Abstract

Animal morphology reflects both evolutionary history and present-day adaptation. Male mammal copulatory structures such as the baculum (penile bone) are ideal for studying these processes because of their complexity and high interspecific variability. In primates, however, research has focused mostly on baculum length. Here we investigate the evolution of primate baculum anatomy and morphology using the largest dataset assembled to date. We combined high-resolution 3D micro-CT reconstructions with advanced non-landmark methods to quantify key traits, including baculum position, discrete shape categories, and a continuous descriptor of overall baculum complexity derived from alpha-shapes analysis. Using stochastic character mapping on a primate phylogeny, we inferred ancestral states and evolutionary transitions for baculum position, shape type, and complexity. Reconstructions indicate that a proximally positioned baculum extending beyond the penile mid-shaft represents the ancestral condition, retained in Strepsirrhini and shifted distally in Haplorrhini. A stick-shaped baculum is inferred as ancestral, with subsequent transitions to Y-shaped and pear-shaped morphologies. Overall, this study provides the first phylogenetically explicit reconstruction of primate baculum evolution, revealing repeated shifts in anatomy and morphology complexity. These results offer a framework for testing functional and selective hypotheses on copulatory structures and highlight the value of 3D morphometrics for understanding morphological diversity across species.

KEYWORDS

alpha-shapes, morphometric techniques, penile bone, phylogenetic analysis, shape complexity

1 | INTRODUCTION

Animal morphology can be understood either as the outcome of its evolutionary history or as an adaptation to its current environment (Bock, 1980; Gotthard & Nylin, 1995). Anatomical forms can be separated into size, shape, texture, color and pattern components (Romer & Parsons, 1996). Among these, shape is arguably one of the most informative features, as it encapsulates critical geometric details beyond simple linear

This is an open access article under the terms of the Creative Commons Attribution License, which permits use, distribution and reproduction in any medium, provided the original work is properly cited.
© 2026 The Author(s). *The Anatomical Record* published by Wiley Periodicals LLC on behalf of American Association for Anatomy.

measurements. Despite its importance, shape has often been overlooked in favor of size, the latter being more straightforward to measure and analyze. However, modern morphometric studies succeed by rigorously quantifying shape, providing new insights into the evolution and diversity of biological forms (Scalici et al., 2018; Spani, Scalici, et al., 2020).

The male copulatory system is subjected to intense selective pressures and evolves more rapidly than other morphological structures ("genitalic extravagance," Eberhard, 1985, 1993; Klaczko et al., 2015). Data accumulation on a broad range of species has progressively dimmed a long-standing debate on the natural versus sexual selection roles in shaping external genitals, now focusing on mechanisms of post-copulatory selection, originally proposed by Eberhard (1985) (see, e.g., Dixson & Anderson, 2001, 2004; Hosken & Stockley, 2004; Simmons, 2014). Understanding the forces behind rapid morphological divergence is key to studying adaptation and speciation processes, and quantifying shape is essential in this context, enabling a more detailed analysis than size alone. Across species with internal fertilization, divergence (i.e., variability) in male genital morphology may be so pronounced that even in closely related, congeneric, and phenotypically similar species male external genitalia can often be used as taxonomic keys (Eberhard, 1985). The baculum (penile bone), in particular, stands out for its extraordinary morphological variability, sometimes with elaborate species-specific morphologies at the distal tip, making it particularly useful for species identification in some taxa (Romer & Parsons, 1996), as, for example, in rodents (Elder & Shanks, 1962; Kankilic et al., 2014; Leon-Alvarado & Ramírez-Chaves, 2017; Patterson & Thaeler, 1982), carnivores (Abramov, 2002; Baryshnikov et al., 2003; Tumlison & McDaniel, 1984), and bats (Benda & Tsytsulina, 2000; Comelis et al., 2015; Herdina et al., 2014). Adaptive hypotheses proposed for the mammalian baculum functions include (a) prolonging intromission while protecting the urethra for successful sperm deposition (the "prolonged intromission hypothesis," Ewer, 1973), (b) stimulating the female reproductive tract/inducing ovulation (the "induced ovulation hypothesis," Greenwald, 1956), and (c) facilitating intromission against vaginal resistance (the "vaginal friction hypothesis," Long & Frank, 1968).

In primates, genital morphology exhibits variation in traits such as penis length and the complexity of the distal portion, including the size and shape of keratinized spines, when present, and the baculum (Dixson, 1987a, 2012; Harcourt & Gardiner, 1994). However, studies on sexually selected traits related to mate choice and competition in mammals, particularly those focusing on genital evolution, have primarily used baculum length as the main quantitative measure of its morphological variation (e.g., Long & Frank, 1968; see Larivière & Ferguson, 2002 and Ferguson & Larivière, 2004 for meta-analyses in carnivorans). At the inter-specific level, baculum length in primates correlates with mean species-specific copulation duration, in line with the prolonged intromission hypothesis (Dixson, 1987a, 1987b; Dixson et al., 2004), and with mating systems (Brindle & Opie, 2016), but not with testis mass, which is commonly used as a proxy for sperm competition intensity and may therefore be relevant to baculum evolution under post-copulatory sexual selection (Brindle & Opie, 2016; Ramm, 2007). Compared to interspecific variation in overall shape (qualitatively described) and size (i.e., length), potentially affected by non-sexual selective forces as well (e.g., Eberhard, 2009), intraspecific polymorphism in the baculum was reported as generally limited (Long & Frank, 1968; Patterson, 1983; Ramm et al., 2010). However, baculum shaft and base width, rather than length, have shown great promise in recent experimental studies on sexual selection, where intra-specific variation correlated with individual reproductive success and sperm competition risk (domestic mice Stockley et al., 2013, Simmons & Firman, 2014; see also Orr & Brennan, 2016 in four mammal orders). Accordingly, a central premise of this study is that baculum shape complexity can provide evolutionary and functional information beyond size alone, because reliance solely on linear measures such as length is likely to oversimplify genital bone variability (Ramm, 2007). This limitation is further compounded by the fact that bacula often lack clear homologous landmarks across taxa, making their morphology difficult to quantify rigorously using traditional landmark-based morphometric approaches.

Beyond primates, baculum research has a long comparative tradition across mammals, particularly in Carnivora, Rodentia, and Chiroptera, where this bone has been investigated not only as a taxonomic character, but also in relation to copulatory behavior, functional mechanics, allometry, and evolutionary diversification (Baryshnikov et al., 2003; Comelis et al., 2015; Elder & Shanks, 1962; Herdina et al., 2014; Patterson & Thaeler, 1982; Tumlison & McDaniel, 1984). In carnivorans in particular, classic systematic work by Didier documented marked interspecific diversity in baculum form across major lineages, including Canidae, Mustelidae, Felidae, Procyonidae, and Ursidae, effectively anticipating the broader comparative perspective that more recent three-dimensional and phylogenetic studies are now able to formalize (Didier, 1946, 1948, 1949, 1950; see also Hartstone-Rose, 2025). More recent analyses in Carnivora and Musteloidea have further shown that baculum morphology preserves both functional and phylogenetic

19328494, 0, Downloaded from https://anatomypubs.onlinelibrary.wiley.com/doi/10.1002/ar.70216 by CochraneItalia, Wiley Online Library on [04/05/2026]. See the Terms and Conditions (https://onlinelibrary.wiley.com/terms-and-conditions) on Wiley Online Library for rules of use; OA articles are governed by the applicable Creative Commons License

information, and that quantitative descriptors of shape complexity can reveal patterns not captured by length alone (Brassey et al., 2020; Clear et al., 2023). Against this broader mammalian background, primates remain comparatively underexplored with respect to fine-scale baculum morpho-anatomy, despite their central importance in debates on baculum evolution and post-copulatory sexual selection.

Advances in digitization and computational methods have revolutionized shape analysis, enabling an improvement in the degree of precise quantification of complex structures. Traditional landmark-based geometric morphometric methods (GMM, Rohlf & Slice, 1990) has long been instrumental in studying a variety of biological shapes from vertebrate skulls (Dumont et al., 2016; Scalici et al., 2018) to insect wings (Ray et al., 2016). GMM is less effective, however, for structures lacking clear homologous points, such the long bones diaphysis (Frelat et al., 2012) and baculum as well. A few studies on the baculum attempted to overcome this limitation and used GMM by applying sliding and surface semi-landmarks (baculum outline shape in Simmons & Firman, 2014; 3D shape in Schultz et al., 2016). Nevertheless, finer-scale geometric differences potentially holding critical evolutionary and functional insights could be investigated only recently, with the development of novel methodologies like generalized procrustes surface analysis (Pomidor et al., 2016), and especially alpha-shapes (Gardiner et al., 2018), the latter being especially formulated for the analysis of complex forms lacking true landmarks. Among the available landmark-free metrics of three-dimensional shape complexity, we selected alpha-shapes because they quantify the overall configurational complexity of the entire structure, are explicitly suited to morphologically diverse forms lacking true homologous landmarks, and have already proven informative in genital bone studies. In addition, alpha-shapes are particularly sensitive to coarse morphological features, especially concavities (Clear et al., 2023), which are highly relevant to baculum form, whereas other metrics such as ariaDNE capture different aspects of surface geometry (Shan et al., 2019). These methods are particularly well-suited to studying genital morphology, whose three-dimensional shape complexity plays a pivotal role in understanding evolutionary patterns (see in carnivores Brassey et al., 2020; Clear et al., 2023). By recognizing that shape, rather than size, better reflects evolutionary forces shaping anatomical structures, the analytical advancements in shape analysis form the foundation of this study.

The primary aim of the present study is to investigate the evolutionary trajectory of baculum anatomy and shape variability by tracing their history and inferring ancestral states in a phylogenetic context. To achieve this, we provide micro-CT scans of male external genitals and baculum specimens derived from published datasets (Spani et al., 2021; Spani, Morigi, et al., 2020) integrated with new original data (and taxa) deriving from fresh samples and museum collections worldwide. By doing so we produced the largest primate baculum database to date. High-resolution 3D reconstructions were used to study the evolutionary pattern of baculum morphology through two complementary levels of description: (a) qualitative observable morphotypes ("stick," "pear," or "Y," as described in Spani, Morigi, et al., 2020), and (b) a continuous landmark-free descriptor of whole-bone three-dimensional complexity obtained through alpha-shape analysis. 3D reconstructions also allowed us to get detailed description of baculum-urethra relative positioning and baculum asymmetry. Based on prior observations (Spani, Morigi, et al., 2020) we hypothesize that anatomical position and shapes dominating in the basal group of Strepsirrhines (i.e., the baculum extending along most of the penis shaft, and the baculum morphotypes described as "stick" or "Y," Spani, Morigi, et al., 2020) reflect the ancestral condition and that, in primates, closely related species exhibit similar baculum shapes due to phylogenetic constraints. The results are discussed primarily in relation to anatomical reconstruction and phylogenetic patterning, while broader functional and selective hypotheses are considered more cautiously as possible interpretive frameworks.

2 | MATERIALS AND METHODS

2.1 | Baculum sampling for micro-CT scans

Micro-CT scanned specimens of primate bacula derived from combining two published datasets ($N = 75$, Spani, Morigi, et al., 2020; Spani et al., 2021) with new original data ($N = 20$), the latter including both extracted bacula ($N = 13$) and penises ($N = 7$; after applying the 3-step protocol checking for baculum presence, see Spani, Morigi, et al., 2020).

Samples were of two kinds: fresh specimens ($N = 14$; all penises) and museum specimens ($N = 81$; 6 entire corpses, 61 penises and 14 bacula). Overall, we collected $N = 95$ specimens (entire corpses, $N = 6$; external genitals, $N = 75$; penile bones, $N = 14$) for 55 primate species and 3 subspecies (S1). These counts refer to the full micro-CT scanned sample reported in S1, which also includes a small number of non-adult specimens. All scanned specimens contributed to the original morpho-anatomical dataset; however, some downstream

19328494, 0, Downloaded from https://anatomypubs.onlinelibrary.wiley.com/doi/10.1002/ar.70216 by CochraneItalia, Wiley Online Library on [04/05/2026]. See the Terms and Conditions (https://onlinelibrary.wiley.com/terms-and-conditions) on Wiley Online Library for rules of use; OA articles are governed by the applicable Creative Commons License

comparative analyses were conducted on analytical subsets only (see below for more details). In particular, when conspecific individuals of different age classes were available, only adults were retained for species-level alpha-shape values, and phylogenetic analyses further included only taxa matching the molecular dataset. Fresh specimens (some of them shown in Figure 1a–f) were obtained opportunistically from primate cadavers before necropsy investigations, in collaboration with several Italian Istituti Zooprofilattici Sperimentali (see Spani, Morigi, et al., 2020 for further details). These animals had died or were euthanized for reasons unrelated to this research. The remaining material consisted of pre-existing museum specimens from zoological collections in Italy, France, and the USA. No primates were euthanized or otherwise procured for the purposes of this study.

Museum specimens were obtained from (1) the Natural History Museum "La Specola" (NHMLS, Florence, IT; Calvini et al., 2016; $N = 8$); (2) The American Museum of Natural History (AMNH, New York, USA; Vertebrate Collection Database available at http://sci-web-001.amnh.org/db/emuwebamnh/index.php; $N = 27$); (3) the National Museum of Natural History (NMNH, Washington, DC, USA; Mammal Collection Database available at https://collections.nmnh.si.edu/search/mammals/; $N = 33$); (4) the Muséum d'Histoire Naturelle de Toulouse where an ancient collection of mammal bacula (dated back to XIX century), and including several primate species (Figure 1g), is available (MHNT, Toulouse, FR; $N = 13$). Either age or age class were recorded whenever available from museum tags or necropsy records, and are reported in S1. However, for most museum specimens, precise age information was unavailable, and many samples consisted of isolated penises or extracted bacula not associated with the whole body. As a result, ontogenetic stage could not be assessed more precisely across most of the dataset. Because ontogenetic variation may affect baculum morphology, age-related effects could not be explicitly modeled in the comparative analyses. To reduce this source of bias, when conspecific individuals of different age classes were available for morphological analyses, only adult specimens were retained for the species-level value used in evolutionary analyses (see below).

2.2 | Qualitative anatomical and morphological dataset acquisition

Qualitative anatomical and morphological data focused on (i) baculum position within the penis and (ii) baculum shape types. Baculum position referred to a binary character trait, whether baculum was either distally located (i.e., restricted to the distal half of the penis) or extended along most of the shaft (i.e., from the glans proximally beyond the mid-shaft of the penis). The baculum shape types referred to the three discrete types—"stick-shaped," "pear-shaped," and "Y-shaped"—outlined primarily on external appearance (inspiring the names) but also on internal structure (see Spani, Morigi, et al., 2020); representative examples are shown in Figure 2 (see below). As an example, pear-shaped bacula consistently displayed a hollow (likely marrow-filled) proximal region combined with a solid distal region, whereas

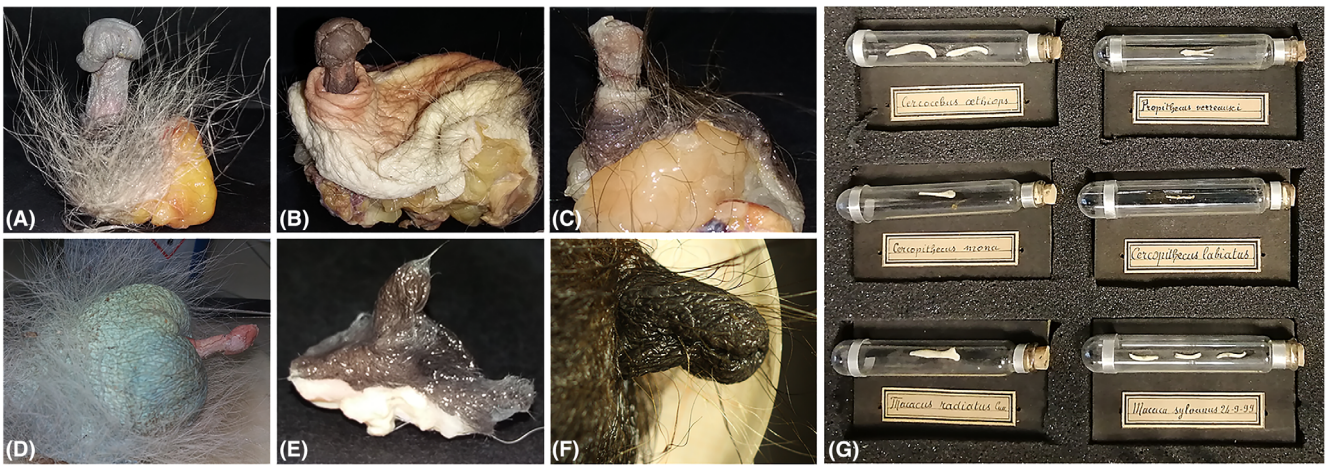

FIGURE 1 (a)–(f) Some external genital samples of male primates used in the present work and provided by different Italian Istituti Zooprofilattici Sperimentali. (a) *Cercopithecus mitis*, adult (ID: 38091); (b) *Macaca fascicularis*, adult (ID: 33031); (c) *Sapajus apella*, adult (ID: 45258); (d) *Chlorocebus pygerithrus*, adult (ID: 55940); (e) *Lemur catta*, infant (ID: 42568); (f) *L. catta*, male (ID: 103729). (g) Detail of the primate baculum collection of Muséum d'Histoire Naturelle de Toulouse (Toulouse, FR) belonging to a collection dated back to the XIX century.

19328494, 0, Downloaded from https://anatomypubs.onlinelibrary.wiley.com/doi/10.1002/ar.70216 by CochraneItalia, Wiley Online Library on [04/05/2026]. See the Terms and Conditions (https://onlinelibrary.wiley.com/terms-and-conditions) on Wiley Online Library for rules of use; OA articles are governed by the applicable Creative Commons License

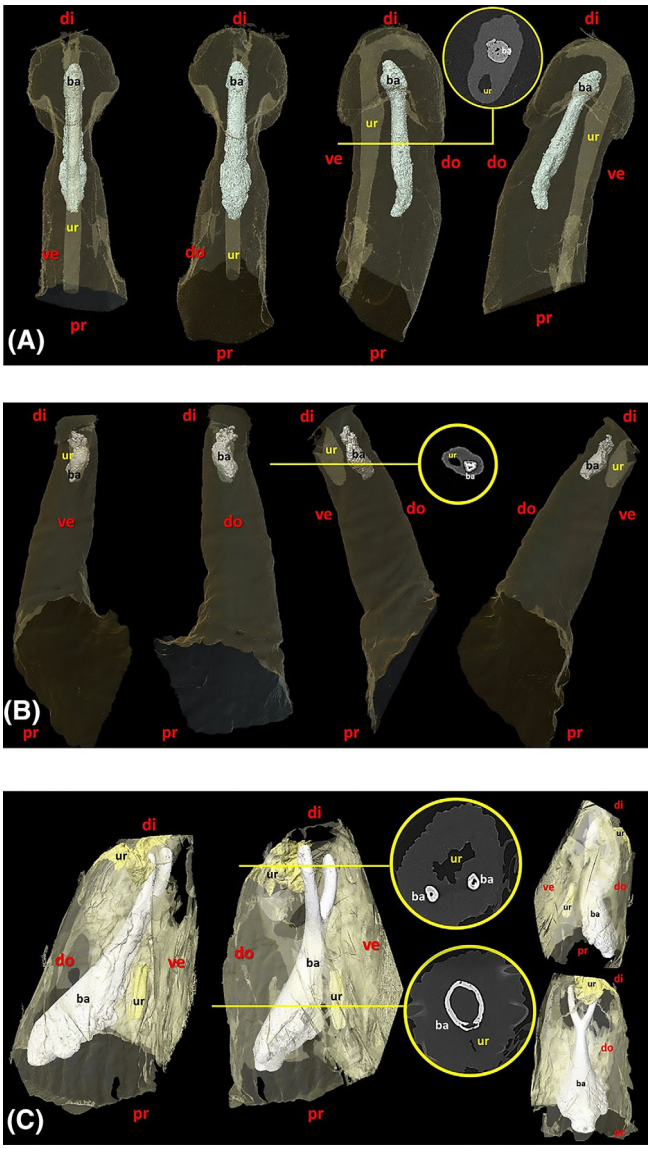

FIGURE 2 External genital 3D reconstruction (penis shaft and glans; light yellow, semi-transparent) of the three morpho-types in adult males of three primate species (a = stick-type: Theropithecus gelada, ID: 269396; b = pear-type: Callithrix jacchus, ID: 267651; c = Y-type: Avahi laniger, ID: 170461). The position of both urethra (ur; yellow, semi-opaque/opaque) and baculum (ba; white, opaque) are shown (di = distal; do = dorsal; pr = proximal; ve = ventral), in 3D models and relative CT-slices (yellow circles).

stick-shaped bacula varied widely in both form (from straight to variably curved) and internal organization, ranging from specimens with a conspicuous internal cavity to specimens appearing compact throughout, with no clearly detectable internal cavity in the Micro-CT scans.

For clarity, four related but distinct datasets were used in this study. First, the original micro-CT scanned sample comprised 95 bacula/specimens from 55 species and 3 subspecies (S1). Second, this original dataset was expanded with literature-derived qualitative observations to build a comparative morpho-anatomical dataset of 104 taxa (95 species and 9 subspecies; S5). Third, because baculum anatomical position could not be coded for all taxa in the qualitative dataset, the position-based comparative matrix included 92 taxa only. Finally, the phylogenetic analyses were conducted on pruned subsets including only taxa represented both in our morphological datasets and in the molecular phylogeny: 84 taxa for baculum position and 95 taxa for qualitative baculum morphotype. The alpha-shape analysis was performed on all 95 scanned meshes, but species-level evolutionary analyses were based on one representative adult-derived optima value per species, yielding 55 species.

Data for the ancestral state reconstruction of baculum anatomical position and qualitative morphotypes were derived from the combined taxon-level dataset summarized above, integrating the original micro-CT sample with additional records compiled from published sources. Because this matrix was coded at the taxon level, the number of taxa does not correspond one-to-one with the number of scanned specimens in the original sample. We conducted an extensive search on historical anatomical papers and electronic peer-reviewed literature, checking the following electronic databases: Scopus, Web of Science and Google Scholar. Keywords searched in all fields (title, author, keywords, text, etc.) were: "baculum" AND "primates," "baculum" AND "shape," "baculum" AND "anatomy," "baculum" AND "position." Data about penile bone position and qualitative shape types extracted from the literature mainly derived from: (a) images or drawings, and (b) explicit mentions in the text. If none of this was available, on a few occasions we inferred them by (c) careful reading of anatomical and morphological descriptions of penis prepuce, shaft, glans, urethra and baculum, sometimes described in their reciprocal anatomical relationships with no explicit mention of bone position and shape, supported by detailed anatomical papers of male external genitalia in non-human species bearing the baculum (e.g., Kelly, 2000). Whenever explicitly reported in the original sources, literature-derived observations were taken from adult male specimens. However, many historical anatomical and museum-based studies did not provide precise age information, and in several cases the published records referred only to extracted bacula or genital preparations, preventing an independent verification of adulthood. For this reason, literature-derived records were not restricted exclusively to known-age adults; instead, only cases in which baculum position and/or qualitative morphotype could be unambiguously coded from figures, drawings, or detailed anatomical descriptions were retained. The resulting literature-augmented dataset spans 14 primate families across Strepsirrhini and Haplorrhini, including

19328494, 0, Downloaded from https://anatomypubs.onlinelibrary.wiley.com/doi/10.1002/ar.70216 by CochraneItalia, Wiley Online Library on [04/05/2026]. See the Terms and Conditions (https://onlinelibrary.wiley.com/terms-and-conditions) on Wiley Online Library for rules of use; OA articles are governed by the applicable Creative Commons License

Platyrrhini and Catarrhini, although Tarsiiformes are not represented.

To obtain baculum anatomical and morpho-type data from the 3D scans, some minimal variations were introduced in the third step of the protocol (see Spani, Morigi, et al., 2020), depending on fresh versus museum specimens and wet versus osteological material. In addition, three different micro-computed tomography systems were used depending on specimen location: the same Italy scanner used by Spani, Morigi, et al. (2020), PHOENIX V|TOME|X S for AMNH specimens, and PHOENIX V|TOME|X M for NMNH specimens. To improve transparency of sample composition and acquisition conditions, scanner/scan-site information is now reported for each scanned specimen in Supplementary Table S1. Methodological adjustments/differences are reported in S2, machine settings are shown in S3, and total time needed to detect and visualize bacula is reported in S4. Because the scanned material combined fresh and museum specimens, wet and osteological material, and acquisitions performed on different micro-CT systems, we cannot completely exclude some effect of preservation state, specimen type, or scanner-specific settings on baculum detectability and segmentation. However, all reconstructed bacula were subsequently processed through the same post-processing and alpha-shape workflow, using standardized mesh treatment and a fixed point-cloud size of 100,000 points.

2.3 | Baculum anatomical analysis

All ancestral state reconstructions present in this study have been using the same and most recent mammalian phylogeny by Álvarez-Carretero et al. (2022). In order to trace the evolutionary history of baculum position in the primate order we used a stochastic character mapping tool (SCM; Nielsen, 2002; Huelsenbeck et al., 2003). For the analysis of baculum anatomical position, we used the subset of the qualitative comparative dataset for which position could be reliably coded (92 taxa). Of these, 84 taxa were also represented in the molecular phylogeny and were therefore retained for stochastic character mapping. Baculum position was coded as a binary trait: "distal" (D) for placement in the distal half of the penis and "extended" (E) for proximal extension beyond the midshaft of the penis. All tip states were assigned as fixed values rather than relative state frequencies, with no uncertainty in their classification. This binary matrix was mapped onto the primate phylogeny to estimate ancestral states and assess the validity of the position pattern described by Spani, Morigi, et al. (2020). Three transition models (Paradis & Schliep, 2019)—Equal rates (ER), Symmetrical (SYM), and all rates different (ARD)—were fitted to the data. Model selection was based on the akaike information criterion (AIC; Posada & Buckley, 2004), with the ARD model yielding the lowest AIC value. Using this model, we estimated the transition matrix (Q matrix) to ensure consistent application of model assumptions. SCM was performed by generating 1000 trees with the binary trait mapped onto them, using the Q matrix from the ARD model for ancestral state reconstruction. The prior distribution of root node frequencies was set to the stationary frequencies of the transition matrix to maintain model consistency. In order to assess the temporal distribution of transition events along the phylogeny, we computed the node heights for each SCM simulation. To assess the phylogenetic signal in baculum position, we applied the D statistic (Fritz & Purvis, 2010), which measures the degree to which a binary trait is phylogenetically conserved, comparing its observed distribution to expectations under a Brownian motion (BM) model ($D = 0$) and a random model ($D = 1$). We used 1000 simulations of trait evolution across phylogenies, generated through SCM, to account for uncertainty in the evolutionary history of the trait. This approach provided a distribution of D values, allowing for a more robust assessment of the phylogenetic signal and the calculation of confidence intervals for more reliable p-value estimation. The observed D statistic was calculated on the original phylogenetic tree, and the p-value was computed by comparing this observed value to the distribution of D values from the simulations. Specifically, the p-value represents the proportion of simulated D values that are greater than or equal to the observed D. This allows us to assess how extreme the observed value is relative to the simulated values and provides a measure of statistical significance. Due to the large number of discrete character histories mapped onto phylogeny, results were aggregated using Method 1 from Revell (2013). This approach involved fractioning tree branches and computing the posterior probability of character transitions as their relative frequency across all stochastic maps. By applying continuous color gradient along branches, posterior probabilities were visually represented. All analyses were conducted using functions from the ape, geiger, phytools, phylobase, caper and phylosignal packages in R. Refer to Data Availability Statement for the complete R code.

2.4 | Baculum qualitative morphological analysis

To reconstruct the evolutionary history of baculum morphology we used the same analytical approach described

19328494, 0, Downloaded from https://anatomypubs.onlinelibrary.wiley.com/doi/10.1002/ar.70216 by CochraneItalia, Wiley Online Library on [04/05/2026]. See the Terms and Conditions (https://onlinelibrary.wiley.com/terms-and-conditions) on Wiley Online Library for rules of use; OA articles are governed by the applicable Creative Commons License

for baculum position. For the analysis of qualitative baculum morphotypes, we used the full literature-augmented qualitative dataset (104 taxa). Of these, 95 taxa were also represented in the molecular phylogeny and were therefore retained for ancestral state reconstruction. Baculum morphology was coded as a multistate trait with three categories: "stick" (S), "pear" (P), and "Y." All tip states were assigned as fixed values rather than relative state frequencies, with no uncertainty in their classification. This matrix was mapped onto the primate phylogeny to estimate the ancestral state of baculum morphology. We fitted the same three transition models (ER, SYM, and ARD) and selected the ER model based on AIC, as it produced the lowest value. The transition matrix (Q matrix) was estimated under this model to maintain consistency in subsequent analyses. SCM was then performed by generating 1000 trees with the mapped trait, using the Q matrix from the ER model for ancestral state reconstruction. The prior distribution of root node frequencies was set to the stationary frequencies of the transition matrix. To assess phylogenetic signal, we estimated Pagel's lambda (Pagel, 1999), which quantifies the extent to which trait variation follows the phylogenetic tree structure ($\lambda = 1$ indicates strong phylogenetic signal, while $\lambda = 0$ suggests lack of phylogenetic signal). To ensure coherence with the uncertainty in trait evolution, λ was calculated using the 1000 trees generated during SCM. The p-values were then calculated by comparing the observed λ value to the distribution of λ values obtained from SCM simulations, and representing the proportion of simulations where $\lambda \geq$ observed λ. All analyses were conducted using functions from the ape, geiger, phytools, phylobase, caper and phylosignal packages in R. Refer to Data Availability Statement for the complete R code.

2.5 | Baculum alpha-shape analysis

To capture additional shape variability not accounted for by the three discrete morpho-types, and further assess the complexity of those qualitative categories, we employed a landmark-free approach known as "alpha-shape" analysis (Gardiner et al., 2018). This technique has been successfully used to evaluate morphological complexity in genital bones of both carnivores and primates (e.g., Brassey et al., 2020; Clear et al., 2023; Spani et al., 2022). Shape complexity was accounted as the degree of sophistication required for the volume of an appropriately fitted "alpha" shape to match the 3D model of a baculum. The applied step-by-step procedure for the post- processing of micro-CT volumes resulting from segmentation, and for performing the alpha-shapes analysis on baculum meshes ($N = 95$), was the same described in detail by Spani et al. (2022); the number of points making up the cloud was set to 100,000. The alpha-shape technique allows to identify the continuous variable $1/k$, the "optimal" refinement (i.e., *optima*), which describes the morphological complexity of a baculum. Briefly, as the value of the refinement coefficient (k) decreases, the percentage of the alpha-shape volume that intersects the CT volume also decreases. Below 100%, the alpha-shape decomposes and traverses the point cloud. On the contrary, excessively high k values correspond to highly coarse alpha-shapes that wrapped the cloud of points adapting only to the outermost points of the cloud itself. The optimal value of k is reached when the volume of the alpha-shape is equal (100%) to the CT volume. Therefore, different shapes of bacula might correspond to different *optima* values. The method proposed by Gardiner et al. (2018) uses the $1/k$ variable as a proxy for shape "complexity" (i.e., alpha complexity) without identifying landmarks therefore overcoming the well-known problem of lack of homologous points in penile bones (Clear et al., 2023). In the present study, optima values were therefore interpreted specifically as a descriptor of whole-bone gross three-dimensional configurational complexity, rather than as a complete proxy for all biologically meaningful aspects of baculum shape.

All tip states were assigned as fixed values rather than relative state frequencies, with no uncertainty in their classification. Alpha-shape analyses were initially performed at the specimen level and subsequently summarized at the species level for phylogenetic analyses. Within the scanned dataset, 16 species were represented by two or more adult specimens, 36 by a single adult specimen, 3 by a mixture of adult and non-adult specimens, and 1 by a non-adult specimen only (see S1). When conspecific specimens of different age classes were available, adult specimens were preferentially retained for the species-level value. In species represented by multiple adult bacula, mean alpha-volume values were calculated across specimens for each k value, and the k corresponding to the mean alpha volume (expressed as a percentage of CT volume) closest to 100% was selected. Because the phylogenetic analyses were conducted on one species-level optima value per species, taxa with more scanned specimens did not contribute disproportionate weight to the macroevolutionary models, although uneven within-species replication may affect the precision of species-level estimates. The software used in the rendering and post-processing phases were Amira, Geomagic Studio 2014 and Meshlab. Alpha-shape analyses were conducted using functions from Rvcg, alphashape3d, RANN, tools packages in R. Refer to Data Availability Statement for the complete R code.

19328494, 0, Downloaded from https://anatomypubs.onlinelibrary.wiley.com/doi/10.1002/ar.70216 by CochraneItalia, Wiley Online Library on [04/05/2026]. See the Terms and Conditions (https://onlinelibrary.wiley.com/terms-and-conditions) on Wiley Online Library for rules of use; OA articles are governed by the applicable Creative Commons License

Optima values were mapped onto the phylogeny and all species present in our dataset ($N = 55$) were included in the analysis. We examined the influence of phylogeny on baculum shape, testing its evolution under either a BM (Wiener, 1923) or Ornstein–Uhlenbeck (OU; Uhlenbeck & Ornstein, 1930) model. In this context, phylogenetic constraints would result in closely related species exhibiting similar baculum shapes, conversely, weak or absent phylogenetic signal would suggest independent shape evolution across species. To assess the best-fitting evolutionary model for the trait, we compared the BM and the OU model with a fixed root, the latter chosen based on AIC values and to ensure numerical stability. To test the presence and strength of phylogenetic signal, Blomberg's K (Blomberg et al., 2003) and Pagel's λ were calculated. These two metrics provide complementary insights: K measures how much the variance in the trait is structured by phylogeny relative to a BM model, while λ quantifies the extent to which the phylogenetic tree explains trait covariance among species. Statistical significance was assessed using permutation tests for K (1000 randomizations) and likelihood ratio tests for λ. Finally, the distribution of baculum *optima* values along the phylogeny was visualized using the contMap function in the Phytools R package (Revell, 2012), which plotted the *optima* values and represented them across the pruned phylogenetic tree.

3 | RESULTS

3.1 | Qualitative morpho-anatomical features of baculum in primates

Micro-CT reconstructions show clear interspecific variation in baculum morphology across primates and also suggest some degree of intraspecific variation (see Figure 5 for 3D reconstructions; see S5 for the qualitative morpho-anatomical dataset built for 104 taxa). However, because exact age information was unavailable for most museum specimens, the relative contribution of ontogeny versus adult individual variation could not be formally disentangled in the present dataset.

As far as the baculum-urethra relative position, in all stick- and pear-type shapes the entire baculum was dorsal to the urethra (Figure 2a,b). Differently, in Y-type shape, only the proximal end of the baculum was dorsal to the urethra, whereas its distal portion reached the urethra sagittal plane, with the two symmetric branches running parallel to it (Figure 2c). Distally, the bone branches showed a slight bending upwards. Moreover, in all stick- and pear-type shapes, the distal end is typically positioned asymmetrically on the left side of the glans, indicating a torsion of the bone along the proximo-distal axis (clearly visible during the segmentation phase in scrollable CT slices; but see figures in Spani, Morigi, et al., 2020).

3.2 | Baculum anatomical ancestral state reconstruction

Baculum anatomical position in the penis was detected as "distal" in $N = 66$ species and $N = 7$ subspecies, whereas "extended" in $N = 19$ species. The observed D statistic (-1.18) is consistent with a phylogenetically structured distribution of baculum position, with closely related species tending to share similar trait states. The distribution of simulated D values had a mean of -1.21 (SD $= 0.0256$), with a 95% confidence interval ranging from -1.258 to -1.155. The observed D value falls within this distribution. However, the associated p-value ($p = 0.08$), calculated as the proportion of simulated D values greater than or equal to the observed D, does not meet the conventional threshold for statistical significance. Therefore, this result is best interpreted as being compatible with phylogenetic conservatism in baculum position, rather than as definitive statistical support for it. In line with this, the observed pattern is clearly nonrandom, whereas its fit to a Brownian expectation suggests strong phylogenetic structuring of the trait. Results of the SCM analysis for baculum anatomical position indicated a mean state change equal to 1 (Figure 3).

Changes were of two kinds: (1) from D to E, equal to zero; (2) from E to D, one time. The mean total time spent in each state was 60% for D trait and 40% for E trait. The posterior probability associated with the root of the tree (100%) supports the reconstruction of a baculum extending beyond the mid-shaft of the penis as the ancestral condition in primates. Then, the ancestral condition evolved into (1) the character transition from E to D (i.e., a baculum distally placed, as shown by the node of Haplorrhini, 99%); (2) the character maintenance in E (i.e., a baculum extending beyond the mid-shaft of the penis, as shown by the node of Strepsirrhini, 100%). Histogram analysis, computed from 1000 SCM simulations, revealed a pronounced peak in transition events at 60–64 million years, indicating a key period of morphological change in baculum positioning (Figure 3) (see S6 for parameter estimates).

3.3 | Baculum qualitative morphological ancestral state reconstruction

Results of the SCM analysis for baculum qualitative morphology indicated at least 5 different state changes

19328494, 0, Downloaded from https://anatomypubs.onlinelibrary.wiley.com/doi/10.1002/ar.70216 by CochraneItalia, Wiley Online Library on [04/05/2026]. See the Terms and Conditions (https://onlinelibrary.wiley.com/terms-and-conditions) on Wiley Online Library for rules of use; OA articles are governed by the applicable Creative Commons License

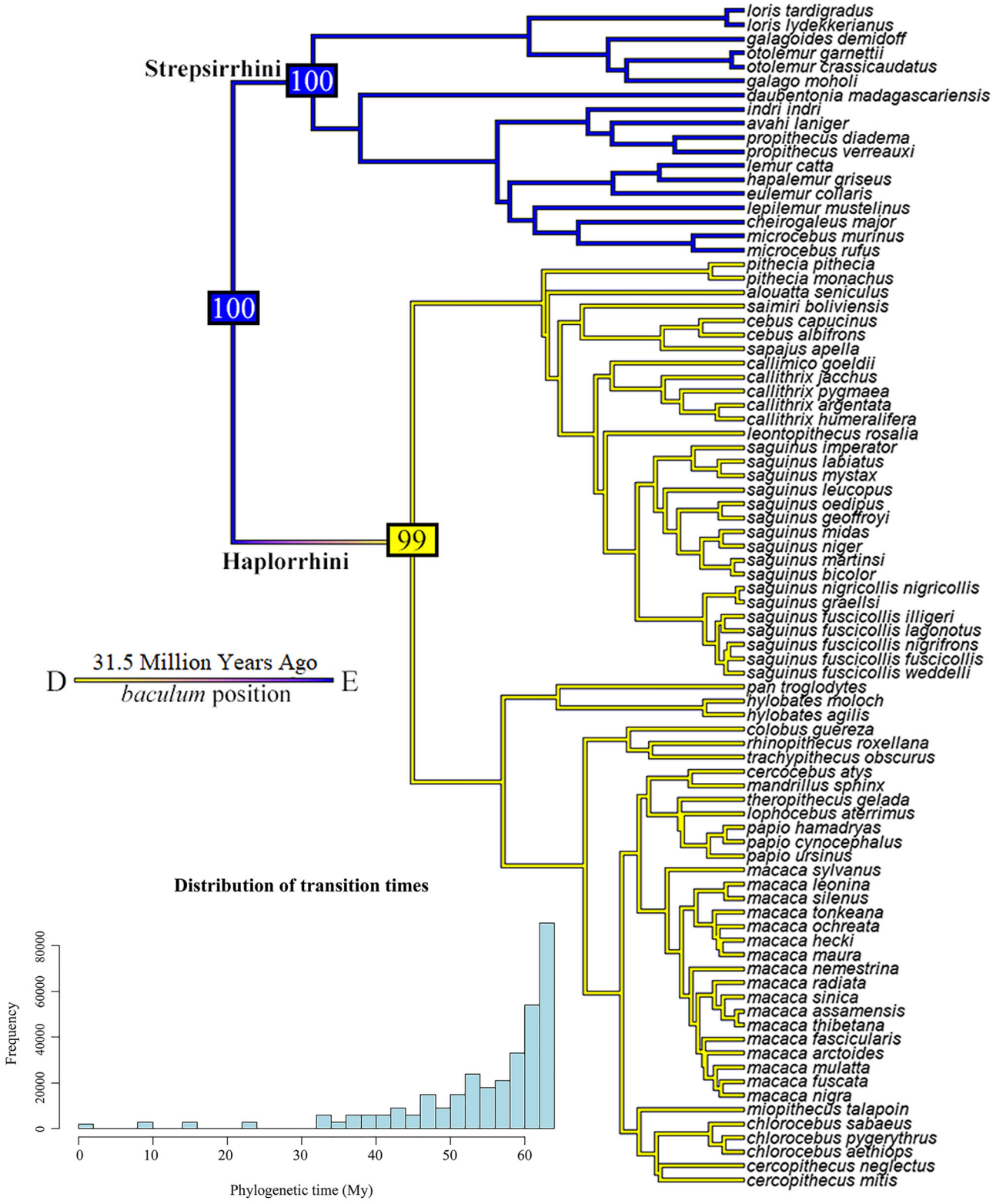

FIGURE 3 Ancestral character state reconstruction of baculum position in primate external genitals. Results from 1000 stochastic character maps displayed in aggregate. The color of edges in the tree gives the posterior probability (computed as the relative frequency across stochastic maps) of each baculum state through the history of the clade. Blue indicates the posterior probability that baculum extends (E) beyond the mid-shaft of the penis, and yellow indicates the posterior probability that baculum is placed in the distal end (D) of the penis; numbers in blue and yellow boxes indicate the proportion of iterations that mapped baculum anatomical position to those branches. The length of the legend gives a scale for the tree branch length (in this case in millions of years ago). Phylogeny by Álvarez-Carretero et al. (2022), pruned. The histogram illustrates the distribution of transition times between baculum positions over phylogenetic time.

19328494, 0, Downloaded from https://anatomypubs.onlinelibrary.wiley.com/doi/10.1002/ar.70216 by CochraneItalia, Wiley Online Library on [04/05/2026]. See the Terms and Conditions (https://onlinelibrary.wiley.com/terms-and-conditions) on Wiley Online Library for rules of use; OA articles are governed by the applicable Creative Commons License

(Figure 4). Changes were of four kinds: (a) from P to S at least one time; (b) from S to P at least one time; (c) from S to Y at least two times, (d) from Y to S at least one time. The mean total time spent in each state was 70% for S trait, 14% for P trait and 16% for Y trait. The posterior probability associated with root node (99%) revealed a high probability that a stick-shape was the baculum ancestral morphological type. For each simulated tree, we estimated the λ value, producing a distribution of λ values. The observed λ value was 1, suggesting a strong phylogenetic influence; however, by comparing the observed λ value to this distribution, the resulting *p*-value was 1, indicating no statistical support for this hypothesis (see S7 for parameter estimates).

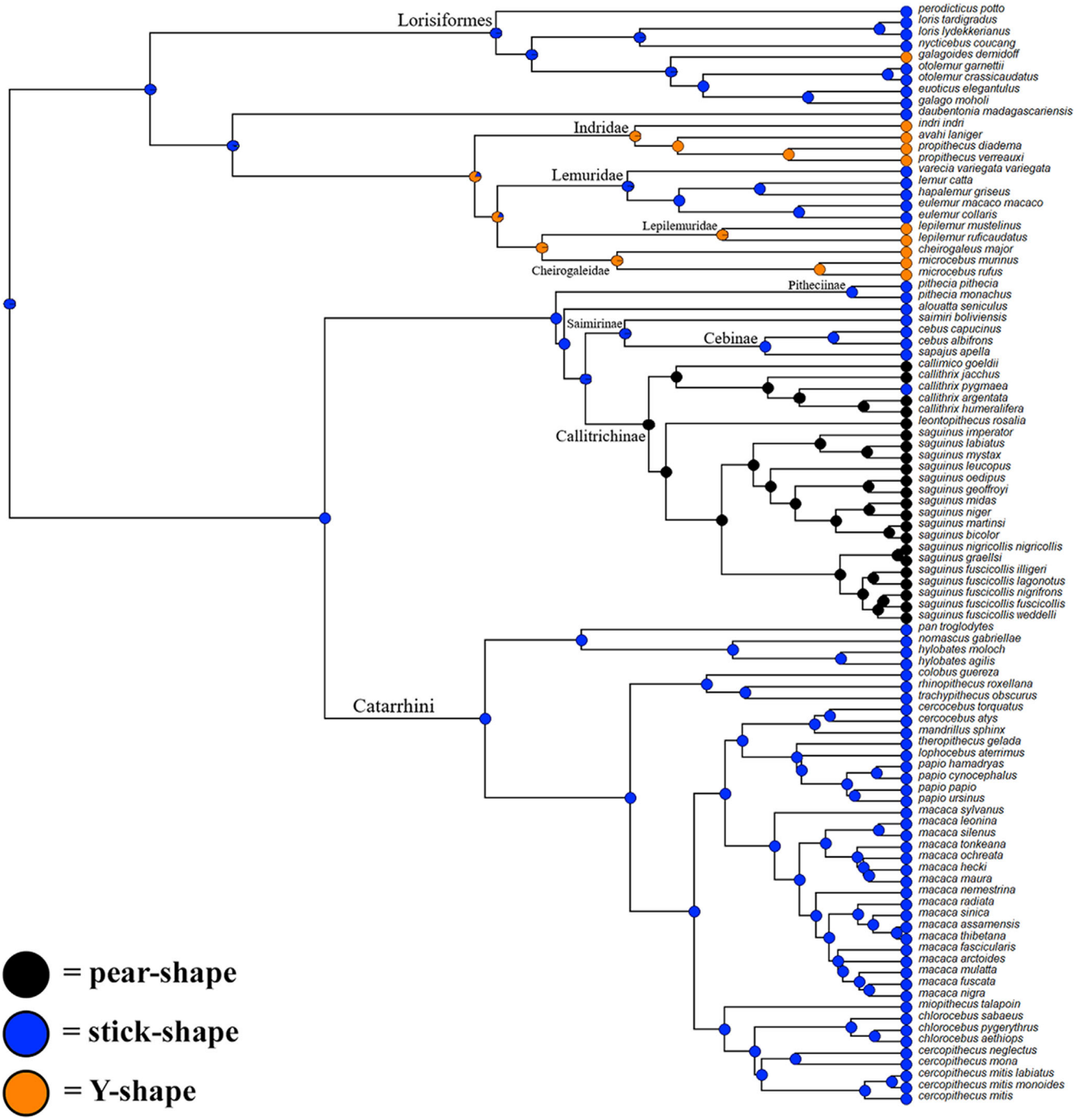

FIGURE 4 Ancestral character estimation of baculum shape state codified as a discrete character. Color of pies at nodes summarized the posterior probabilities that each node is in each state. Pie colors at the tips stand for different baculum shapes: Blue is for stick-shape (S), black is for pear-shape (P) and orange is for Y-shape (Y). Álvarez-Carretero et al. (2022), pruned.

19328494, 0, Downloaded from https://anatomypubs.onlinelibrary.wiley.com/doi/10.1002/ar.70216 by CochraneItalia, Wiley Online Library on [04/05/2026]. See the Terms and Conditions (https://onlinelibrary.wiley.com/terms-and-conditions) on Wiley Online Library for rules of use; OA articles are governed by the applicable Creative Commons License

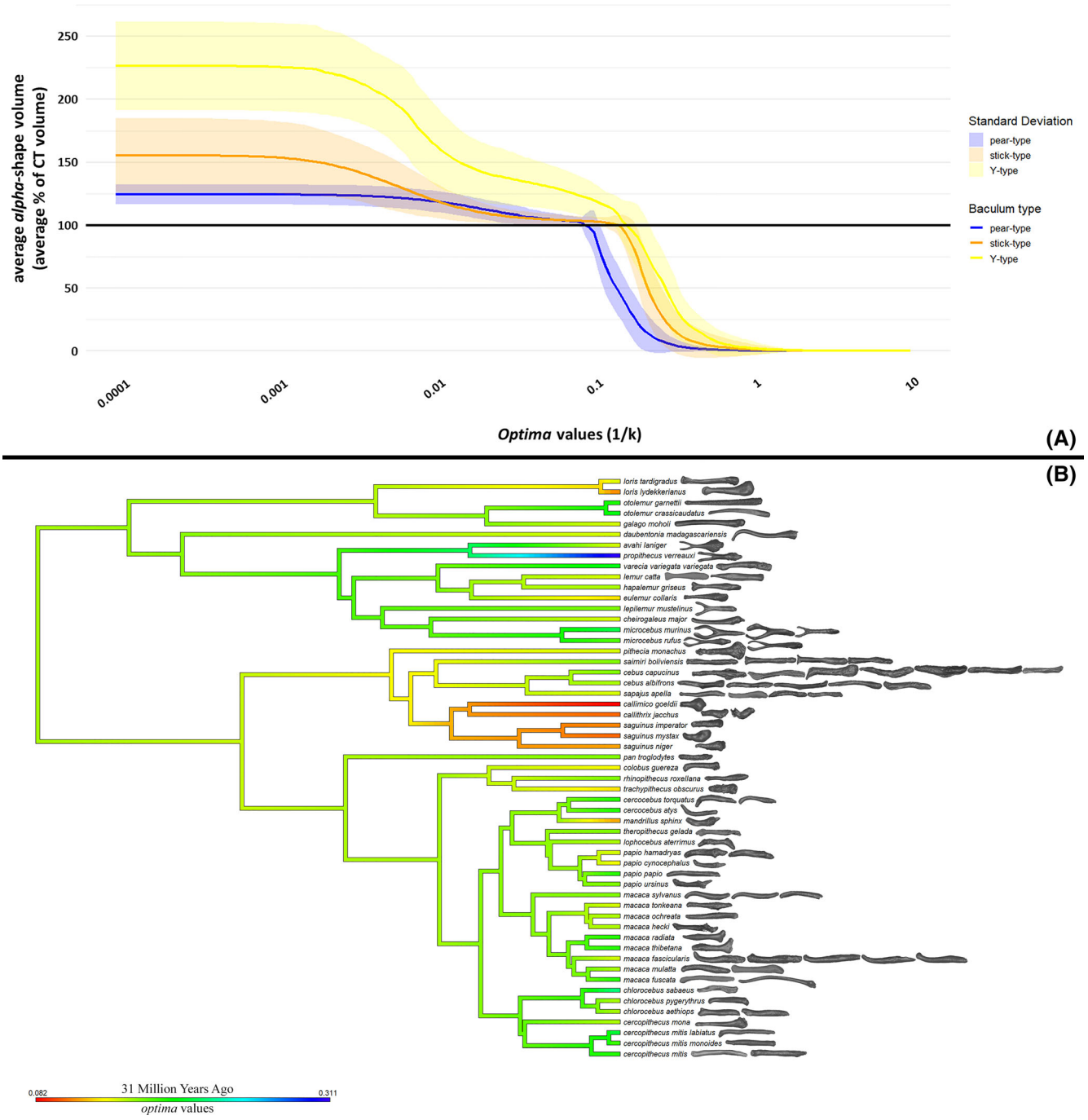

FIGURE 5 (a) Average alpha-shape curves for each baculum morphotype, showing optima values versus the percentage of CT volume described. Shaded areas indicate standard deviation. The black horizontal line marks the point at which alpha-curves reach 100% of the CT volume, identifying the optima value for each morphotype. (b) Ancestral character estimation of baculum optima values across the pruned primate phylogeny. Branch color represents whole-bone alpha-shape complexity, from lower values (red) to higher values (green to blue). Three-dimensional baculum reconstructions are mapped to the corresponding terminal taxa for the scanned species included in the micro-CT dataset, shown in standardized lateral view, with the proximal end to the left and the distal end to the right. Reconstructions are not to scale. Phylogeny after Álvarez-Carretero et al. (2022), pruned to match the taxa included in the analysis.

3.4 | Alpha-shape complexity ancestral state reconstruction

The alpha-shape analysis (quantitative morphology) summarized the shape complexity of each 3D scanned baculum into a single curve. The technique produced as many curves as scanned bacula (curves in aggregation, see graph S8), and the detection of similar trends (i.e., similar baculum shapes, whether stick, pear, or Y) for all alpha-shape turned out to be difficult (for alpha-

19328494, 0, Downloaded from https://anatomypubs.onlinelibrary.wiley.com/doi/10.1002/ar.70216 by CochraneItalia, Wiley Online Library on [04/05/2026]. See the Terms and Conditions (https://onlinelibrary.wiley.com/terms-and-conditions) on Wiley Online Library for rules of use; OA articles are governed by the applicable Creative Commons License

shapes volumes, corresponding measurement error data and *optima* values see S9). To quantify baculum morpho-type alpha complexity we calculated the average "optimal" refinement (i.e., *optima*, $1/k$) for each morpho-type to obtain averaged alpha-shape curves, and corresponding standard deviation. The result (Figure 5a) shows that the *optima* value associated with the Y-type is the highest (*optima* = 0.165), indicating the greatest morphological complexity, followed by the *optima* value of the stick-type (*optima* = 0.147), and finally the *optima* value of the pear-type (*optima* = 0.092), which corresponds to the lowest morphological complexity. These results indicate that whole-bone alpha-shape optima can summarize broad differences in overall baculum complexity, but they should not be interpreted as a one-to-one descriptor of qualitative morphotype identity.

The K statistics revealed a moderate and significant phylogenetic signal ($K = 0.29$; $p = 0.004$), suggesting that closely related species tend to have more similar *optima* values than expected under random evolution. Pagel's λ was 0.83 ($p = 0.0049$), indicating a strong phylogenetic signal with a statistically significant relationship between phylogeny and the trait values. The reconstructed *optima* value for the common ancestor of Primates was 0.16. The distribution of baculum *optima* values were visualized along the phylogeny using the contMap function in the Phytools R package (Figure 5b). The continuous gradient of *optima* values was represented across the pruned phylogenetic tree, where red represented species with low baculum morphological complexity, and blue represented species with higher complexity.

4 | DISCUSSION

By integrating literature with original micro-CT data from museum collections and fresh samples, we assembled an expanded comparative dataset for primate baculum anatomy and morphology. Using SCM and landmark-free shape analysis, we reconstructed broad evolutionary patterns in baculum position, qualitative morphotype, and overall baculum complexity. The main results can be summarized as follows: (a) primate bacula vary interspecifically in both anatomical position within the penis and external/internal morphology; (b) the ancestral baculum most likely extended beyond the penile mid-shaft, a condition retained in Strepsirrhini but replaced by a distally positioned baculum in the sampled Simiformes; and (c) the ancestral baculum shape was most likely stick-like, with later transitions giving rise to Y-shaped and pear-shaped morphologies in specific clades.

An important limitation of the present study concerns intraspecific and ontogenetic variation. Although specimen age was reported whenever available, precise age data were unavailable for most museum specimens, and many samples consisted of isolated genital material or extracted bacula not associated with the whole body, precluding a more accurate age assessment. Therefore, the effect of ontogeny on baculum morphology could not be systematically tested across taxa. This is relevant because baculum robusticity, curvature, and overall shape may vary within species, and part of this variation may reflect developmental stage rather than taxonomic divergence. Accordingly, species represented by one or few individuals should be interpreted with caution, as some portion of the observed interspecific variation may overlap with unsampled intraspecific variation. Future work based on age-known ontogenetic series and broader within-species sampling will be essential to disentangle developmental from evolutionary patterns. An additional limitation of the alpha-shape dataset is that within-species replication is uneven across taxa. Although this does not overweight better-sampled species in the phylogenetic analyses, because each species contributes only one species-level optima value, it does affect the confidence with which species-level complexity estimates can be generalized in poorly sampled taxa.

Micro-CT images revealed that the urethra is placed ventrally in both stick- and pear-shape bacula which, however, did not show urethra-related morphological specializations as seen in Carnivora. In fact, urethra-related baculum specializations are well documented in Carnivora, but their distribution is more heterogeneous than a single family-level pattern would suggest. In Mustelidae, bacular morphology is highly variable and a urethral groove is not universally present across taxa, the ancestral condition being an elongated rod-like baculum lacking a groove (Baryshnikov et al., 2003; Didier, 1948). In Canidae, by contrast, a ventral urethral groove has been described in the Eurasian wolf and more broadly characterizes several canids (Brassey et al., 2020; Čanády & Čomor, 2013; Didier, 1946). Felids also provide a relevant comparative context, as they possess ossified bacula that, although generally much shorter and simpler than those of many other carnivorans, may still offer informative comparisons in overall form (Didier, 1949; Tumlison & McDaniel, 1984; Hartstone-Rose, 2025). Conversely, primate bacula mirror Lagomorpha (Weimann et al., 2014), and some European moles (Talpidae; Nedyalkov et al., 2021) bacula that vary in shape (cylindrical with considerable morphological variation at proximal and distal ends in the former; either straight and slightly curved on the right or sinuate in the latter) but lack any urethra-related specialization. Finally, in Y-shaped bacula, moving from proximal to distal end of the penis, the urethra shifts from a ventral to a dorsal position, passing through the baculum's bifurcation. A

19328494, 0, Downloaded from https://anatomypubs.onlinelibrary.wiley.com/doi/10.1002/ar.70216 by CochraneItalia, Wiley Online Library on [04/05/2026]. See the Terms and Conditions (https://onlinelibrary.wiley.com/terms-and-conditions) on Wiley Online Library for rules of use; OA articles are governed by the applicable Creative Commons License

similar trend occurs in Chiroptera, where the forked distal baculum enclosed the dorsal half of urethra (Herdina et al., 2015).

A general deviation from the bilateral symmetry has been observed in most of the sampled bacula whose distal end showed a slight torsion toward the left side of glans. This may be justified by the baculum anatomical relationships with urethra and surrounding soft tissues, as previously noted in a baculum sample of *Mandrillus sphinx* (Linnaeus 1758) by Spani, Morigi, et al. (2020). Most interestingly, some studies reported a general asymmetry also of penis glans (Hill, 1966, 1974; Pocock, 1918) with an enlargement of the glans left lobe containing the baculum and corresponding to a urinary meatus skewed to the right (Cebidae and most Cercopithecidae, Hill, 1966, 1974; some "anthropoids," Hershkovitz, 1977, 1993). Glans asymmetry still persists in species with a highly reduced or absent baculum, such as *Aotus*, *Lagothrix*, and *Ateles* (Hershkovitz, 1977, 1993).

In a variety of strepsirrhine species possessing an elongated baculum, Dixson (1987a) described the distal portion of the bone extending slightly past the urethral opening during erection. Although several authors described baculum position within penile soft tissues in detail (Hershkovitz, 1977, 1993; Hill, 1974; Matthews, 1946; Pocock, 1918), none explicitly identified a positional pattern congruent with the Strepsirrhini–Haplorrhini distinction, apart from Spani, Morigi, et al. (2020). Our ancestral-state reconstruction provides phylogenetic support for this broader pattern, indicating an extended baculum as the ancestral condition in primates and a shift toward distal confinement along the haplorrhine lineage between 64 and 60 MYA, broadly consistent with current estimates for the Strepsirrhini–Haplorrhini divergence (Pozzi et al. 2014; Shao et al., 2023; Craig et al., 2024). In this sense, the present results provide explicit comparative support for the evolutionary framework previously proposed by Dixson (1987b, 2012, see also Martin 2007), according to which relative baculum length and position in primates may reflect both phylogeny and reproductive biology.

These anatomical reconstructions can be considered in light of broader hypotheses proposed for baculum evolution in primates, including possible relationships with mating system, prolonged intromission, and post-copulatory sexual selection (Brindle & Opie, 2016; Dixson, 1987a, 1987b,1995, 2012; Dixson et al., 2004; Martin, 2007). However, these correlates were not directly tested in the present study and should therefore be treated as interpretive scenarios rather than as supported causal explanations of the observed patterns. In primates, longer bacula have been associated with prolonged intromission and with mating systems involving more intense post-copulatory sexual selection, potentially because an extended baculum may provide mechanical support, facilitate sperm transfer, protect the urethra, and maintain post-ejaculatory intromission (Dixson, 1987a, 1987b, 2012; Dixson et al., 2004; Stockley, 2012; Herdina et al., 2015; Brindle & Opie, 2016). In the strepsirrhine taxa for which behavioral data are available, copulation can indeed be prolonged (Dixson, 1987b; Nekaris, 2003; Tardif et al., 2012), but these associations should not be generalized uniformly across the suborder. Fossil evidence nevertheless suggests that an enlarged baculum may be evolutionarily ancient in primates: two fossil specimens of *Europolemur kelleri* (Middle Eocene, ca. 48 MYA) have been described as possessing an enlarged baculum (Koenigswald, 1979, 1985; Dixson, 1987a, 1987b; Franzen et al., 2009; Boyer et al., 2013). These hypotheses should therefore be regarded as comparative context for the anatomical reconstructions presented here, rather than as direct conclusions of the present study.

These primate patterns should also be interpreted within the broader comparative literature on mammalian bacula. In carnivorans, decades of anatomical and systematic work have shown that baculum morphology can retain species-diagnostic, phylogenetically informative, and functionally relevant variation, from the classic comparative syntheses of Didier to more recent studies based on three-dimensional shape analyses and complexity metrics (Baryshnikov et al., 2003; Brassey et al., 2020; Clear et al., 2023; Didier, 1946, 1948, 1949, 1950; Hartstone-Rose, 2025). In this sense, the present study extends to Primates a broader comparative framework that has already proven informative in other mammalian clades, while highlighting that primate baculum research has so far remained more strongly centered on length than on detailed morpho-anatomical and shape-based variation.

To investigate the evolutionary interplay between baculum shape and its variation in primates, we first reconstructed the ancestral state of three discrete shape conditions (the stick-, pear-, and Y-morpho-types) and, to complement the qualitative observations, we reconstructed the ancestral state of shape complexity as a continuous variable (*optima* values). Overall, although with a different strength, both morphological phylogenetic analyses suggested the stick-shaped baculum as ancestral. Although two out of three morpho-types turned out to be distinctive of two clades (the Y-shape for the Strepsirrhine and the pear-type for the Callithricinae), the analysis on the discrete morpho-types showed no significant phylogenetic signal and combined with the simplicity of the best-supported model ER model—assuming uniform transition probabilities between states—provided no phylogenetic structuring. On the contrary, when shape complexity was more properly captured by a qualitative

19328494, 0, Downloaded from https://anatomypubs.onlinelibrary.wiley.com/doi/10.1002/ar.70216 by CochraneItalia, Wiley Online Library on [04/05/2026]. See the Terms and Conditions (https://onlinelibrary.wiley.com/terms-and-conditions) on Wiley Online Library for rules of use; OA articles are governed by the applicable Creative Commons License

continuous descriptor, phylogenetic analysis was more informative on shape evolution, and despite a moderate signal, phylogeny significantly explained at least part of the variance observed (see later for additional considerations). Although a comparison between 3D shape complexity metrics versus a qualitative scoring method lies beyond the scope of this study, we nevertheless acknowledge that, based on our phylogenetic results, the distribution of baculum discrete morphotypes among primates may represent too coarse a measure to detect evolutionary patterns, thereby underscoring the critical value of advanced, morphometric, non-landmark-based approaches. Tracing further back in evolutionary time, middle Eocene Adapiformes' images/drawings showed large bacula that were neither stick-shaped, nor pear-shaped, nor Y-shaped, but instead exhibited a straight and long diaphysis with large bumps at both epiphyses, and no bilateral symmetry. Their morphology was overall more similar to bacula of Lorisiformes (specifically *Loris* genus) than to those found in more closely related Lemuriformes.

Whole-bone alpha-shape analysis provided a continuous summary of broad baculum configurational complexity across primates, complementing the discrete morphotype classification by capturing variation not reducible to length alone and allowing evolutionary analyses on a continuous trait. However, its biological interpretation must remain scale-specific. In our dataset, the whole-bone approach did not reliably separate two qualitatively distinct morphotypes, namely the stick-type and the Y-type, indicating that optima values should not be interpreted as a complete proxy for baculum form. Rather, they appear to capture gross aspects of structure-wide complexity while being less sensitive to localized features that may nevertheless be morphologically and biologically meaningful. This interpretation is consistent with previous studies applying alpha-shapes to genital bones. In carnivorans and musteloids, analyses conducted separately on baculum subregions along the long axis showed that distal-tip complexity can be more informative than global estimates, revealing patterns otherwise not captured by the global approach (Brassey et al., 2020; Clear et al., 2023). In addition, distal-tip alpha-shape complexity was found to correlate positively with post-copulatory selection proxies, in agreement with the prolonged intromission and induced copulation hypotheses (Brassey et al., 2020; Clear et al., 2023; Ewer, 1973; Greenwald, 1956). Likewise, comparisons between alpha-shapes and ariaDNE, coupled with qualitative shape scoring, showed that these methods are sensitive to different scales of morphology, with ariaDNE better capturing fine-scale topographic features such as distal bifurcations, and alpha-shapes better capturing grooves, bends, concavities, and other coarse aspects of overall shape (Clear et al., 2023; Gardiner et al., 2018; Shan et al., 2019). Accordingly, the present optima values are best interpreted as a first continuous descriptor of overall primate baculum complexity, whereas future analyses focused on subregions, especially the distal tip, will likely be necessary to resolve more localized biologically meaningful shape contrasts.

Even so, identifying which primate species exhibit similar reconstructed *optima* value of 0.16, it is worth clarifying that out of 8 species classified as stick-shaped baculum species (*Cebus capucinus*, *Lepilemur mustelinus*, *Macaca sylvanus, Pan troglodytes*, *Papio ursinus*, *Rhinopithecus roxellana*, *Saimiri boliviensis*, *Theropithecus gelada*), only 1 (*L. mustelinus*) has a Y-shaped baculum.

This study provides the most comprehensive primate baculum morpho-anatomical dataset assembled to date and offers the first phylogenetically explicit reconstruction of baculum position, qualitative morphotype distribution, and overall baculum complexity in Primates. Taken together, the qualitative and quantitative analyses are consistent with a simple ancestral baculum morphology extending beyond the penile mid-shaft, followed by repeated evolutionary shifts in both position and shape complexity across primate clades. Although the present analyses do not directly test functional or selective correlates, they establish a robust comparative framework for future studies examining the relationship between baculum morphology, reproductive biology, and ecological variables across primate lineages.

AUTHOR CONTRIBUTIONS

Morigi Maria Pia: Methodology; software; data curation; resources; writing – review and editing. **Federica Spani:** Methodology; software; data curation; investigation; validation; formal analysis; visualization; conceptualization; writing – original draft; writing – review and editing. **Bettuzzi Matteo:** Methodology; software; data curation; resources; writing – review and editing. **Carosi Monica:** Project administration; writing – review and editing; supervision.

ACKNOWLEDGMENTS

We are in debt with all the veterinarians at Italian Istituti Zooprofilattici Sperimentali of different Italian Districts, who provided fresh samples (Dr. Luca Gelmini and Dr. Maria Cristina Fontana, IZSLER-Modena and Bologna, Lombardy and Emilia-Romagna Districts, IT; Dr. Claudia Eleni, IZSLT-Ciampino, Lazio and Tuscany Districts, IT; Dr. Cristina Biolatti, IZSTO-Torino, Piedmont, Liguria and Aosta Valley Districts, IT; Dr. Eliana Schiavon, IZSVE-Lagnaro, Trentino-South Tyrol, Veneto and Friuli-Venezia Giulia Districts, IT). We are also in debt with: Dr. Francesca Mazzeo (Roma, IT) health director of Veterinary Clinic

19328494, 0, Downloaded from https://anatomypubs.onlinelibrary.wiley.com/doi/10.1002/ar.70216 by CochraneItalia, Wiley Online Library on [04/05/2026]. See the Terms and Conditions (https://onlinelibrary.wiley.com/terms-and-conditions) on Wiley Online Library for rules of use; OA articles are governed by the applicable Creative Commons License

"Enrico Fermi," for allowing to use her personal radiography (X-Ray) machine; Dr. Paolo Agnelli (NHMLS-Firenze, IT) mammalian collection curator of Natural History Museum of "La Specola" in Florence (Italy), for the permission to apply a destructive sampling to ancient specimens of museum wet primate collection; Dr. Lu Yao, Dr. Ross MacPhee (AMNH-New York, USA), Dr. Darrin Lunde and Dr. Scott Whittacker (NMNH-Washington, DC, USA) for the precious support in accessing, exploring and scanning museum samples. Open access publishing facilitated by Universita Campus Bio-Medico di Roma, as part of the Wiley - CRUI-CARE agreement.

DATA AVAILABILITY STATEMENT

The data that support the findings of this study are openly available in Zenodo at https://doi.org/10.5281/zenodo.19226576.

ORCID

Federica Spani https://orcid.org/0000-0001-9577-8875
Maria Pia Morigi https://orcid.org/0000-0001-5697-2325
Matteo Bettuzzi https://orcid.org/0000-0003-3464-6574
Monica Carosi https://orcid.org/0000-0003-1377-2942

REFERENCES

Abramov, A. V. (2002). Variation of the baculum structure of the Palaearctic badger (Carnivora, Mustelidae, *Meles*). *Russian Journal of Theriology*, *1*(1), 57–60.

Álvarez-Carretero, S., Tamuri, A. U., Battini, M., Nascimento, F. F., Carlisle, E., Asher, R. J., Yang, Z., Donoghue, P. C. J., & Dos Reis, M. (2022). A species-level timeline of mammal evolution integrating phylogenomic data. *Nature*, *602*(7896), 263–267.

Baryshnikov, G. F., Bininda-Emonds, O. R. P., & Abramov, A. V. (2003). Morphological variability and evolution of the baculum (os penis) in mustelidae (Carnivora). *Journal of Mammalogy*, *84*(2), 673–690.

Benda, P., & Tsytsulina, K. (2000). Taxonomic revision of *Myotis mystacinus* group (Mammalia: Chiroptera). *Acta Societatis Zoologicae Bohemicae*, *64*, 331–398.

Blomberg, S. P., Garland, T., & Ives, A. R. (2003). Testing for phylogenetic signal in comparative data: behavioral traits are more labile. *Evolution*, *57*(4), 717–745.

Bock, W. J. (1980). The definition and recognition of biological adaptation. *American Zoologist*, *20*(1), 217–227.

Boyer, D. M., Yapuncich, G. S., Chester, S. G., Bloch, J. I., & Godinot, M. (2013). Hands of early primates. *American Journal of Physical Anthropology*, *152*, 33–78.

Brassey, C. A., Behnsen, J., & Gardiner, J. D. (2020). Postcopulatory sexual selection and the evolution of shape complexity in the carnivoran baculum. *Proceedings of the Royal Society B*, *287*(1936), 20201883.

Brindle, M., & Opie, C. (2016). Postcopulatory sexual selection influences baculum evolution in primates and carnivores. *Proceedings of the Royal Society B*, *283*(1844), 20161736.

Calvini, M., Siori, M. S., Gippoliti, S., & Pavia, M. (2016). Catalogue of the primatological collection of the Torino University. *Natural History Sciences*, *3*(2), 3–26.

Čanády, A., & Čomor, L. (2013). Contribution to the knowledge of variability of the penis bone (baculum) in *Canis lupus* from Slovakia (Carnivora: Canidae). *Lynx*, *44*, 5–12.

Clear, E., Grant, R., Gardiner, J., & Brassey, C. (2023). Baculum shape complexity correlates to metrics of post-copulatory sexual selection in Musteloidea. *Journal of Morphology*, *284*(4), e21572.

Comelis, M. T., Bueno, L. M., Góes, R. M., & Morielle-Versute, E. (2015). Penile histomorphology of the Neotropical bat *Eptesicus furinalis* (Chiroptera: Vespertilionidae). *Zoologischer Anzeiger*, *258*, 92–98.

Craig, J. M., Hedges, S. B., & Kumar, S. (2024). Completing a molecular timetree of primates. *Frontiers in Bioinformatics*, *4*, 1495417.

Didier, R. (1946). Etude systematique de l'os penien des mammiferes: Carnivores, Canides. *Mammalia*, *10*, 78–91.

Didier, R. (1948). Etude systematique de l'os penien des mammiferes: Famille des Mustelides. *Mammalia*, *11–12*, 30–43. 139–152, 167–193.

Didier, R. (1949). Etude systematique de l'os penien des mammiferes: Famille des Felides. *Mammalia*, *13*, 17–37.

Didier, R. (1950). Etude systematique de l'os penien des mammiferes: Procyonides. Ursides. *Mammalia*, *14*, 78–94.

Dixson, A., & Anderson, M. (2001). Sexual selection and the comparative anatomy of reproduction in monkeys, apes, and human beings. *Annual Review of Sex Research*, *12*(1), 121–144.

Dixson, A., Nyholt, J., & Anderson, M. (2004). A positive relationship between baculum length and prolonged intromission patterns in mammals. *Acta Zoologica Sinica*, *50*, 490–503.

Dixson, A. F. (1987a). Observations on the evolution of the genitalia and copulatory behaviour in male primates. *Journal of Zoology*, *213*(3), 423–443.

Dixson, A. F. (1987b). Baculum length and copulatory behavior in primates. *American Journal of Primatology*, *13*(1), 51–60.

Dixson, A. F. (1995). Baculum length and copulatory behaviour in carnivores and pinnipeds (Grand Order Ferae). *Journal of Zoology*, *235*(1), 67–76.

Dixson, A. F. (2012). *Primate sexuality: comparative studes of the prosimians, monkeys, apes, and human beings* (2nd ed.). Oxford University Press.

Dixson, A. F., & Anderson, M. J. (2004). Sexual behavior, reproductive physiology and sperm competition in male mammals. *Physiology & Behavior*, *83*(2), 361–371.

Dumont, M., Wall, C. E., Botton-Divet, L., Goswami, A., Peigné, S., & Fabre, A.-C. (2016). Do functional demands associated with locomotor habitat, diet, and activity pattern drive skull shape evolution in musteloid carnivorans? *Biological Journal of the Linnean Society*, *117*(4), 858–878.

Eberhard, W. G. (1985). *Sexual selection and animal genitalia*. Harvard University Press.

Eberhard, W. G. (1993). Evaluating models of sexual selection: genitalia as a test case. *American Naturalist*, *142*(3), 564–571.

Eberhard, W. G. (2009). Static allometry and animal genitalia. *Evolution*, *63*(1), 48–66.

Elder, W. H., & Shanks, C. E. (1962). Age changes in tooth wear and morphology of the baculum in 557 muskrats. *Journal of Mammalogy*, *43*(2), 144–150.

19328494, 0, Downloaded from https://anatomypubs.onlinelibrary.wiley.com/doi/10.1002/ar.70216 by CochraneItalia, Wiley Online Library on [04/05/2026]. See the Terms and Conditions (https://onlinelibrary.wiley.com/terms-and-conditions) on Wiley Online Library for rules of use; OA articles are governed by the applicable Creative Commons License

Ewer, R. F. (1973). *The carnivores*. Cornell University Press.

Ferguson, H., & Larivière, S. S. (2004). Are long penis bones an adaption to high latitude snowy environments? *Oikos*, *105*(2), 255–267.

Franzen, J. L., Gingerich, P. D., Habersetzer, J., Hurum, J. H., von Koenigswald, W., & Smith, B. H. (2009). Complete primate skeleton from the Middle Eocene of Messel in Germany: morphology and paleobiology. *PLoS One*, *4*(5), e5723.

Frelat, M. A., Katina, S., Weber, G. W., & Bookstein, F. L. (2012). Technical note: a novel geometric morphometric approach to the study of long bone shape variation. *American Journal of Physical Anthropology*, *149*(4), 628–638.

Fritz, S. A., & Purvis, A. (2010). Selectivity in mammalian extinction risk and threat types: A new measure of phylogenetic signal strength in binary traits. *Conservation Biology*, *24*(4), 1042–1051.

Gardiner, J. D., Behnsen, J., & Brassey, C. A. (2018). Alpha shapes: determining 3D shape complexity across morphologically diverse structures. *BMC Evolutionary Biology*, *18*(1), 184.

Gotthard, K., & Nylin, S. (1995). Adaptive plasticity and plasticity as an adaptation: a selective review of plasticity in animal morphology and life history. *Oikos*, *74*(1), 3–17.

Greenwald, G. S. (1956). The reproductive cycle of the field mouse, *Microtus californicus*. *Journal of Mammalogy*, *37*(2), 213–222.

Harcourt, A. H., & Gardiner, J. (1994). Sexual selection and genital anatomy of male primates. *Proceedings of the Royal Society of London. Series B, Biological Sciences*, *255*(1342), 47–53.

Hartstone-Rose, A. (2025). Commentary: The missing sabertooth baculum—At what point might the absence of evidence reasonably be considered evidence of absence? *The Anatomical Record*, *308*(11), 3053–3062.

Herdina, A. N., Hulva, P., Horáček, I., Benda, P., Mayer, C., Hilgers, H., & Metscher, B. D. (2014). MicroCT imaging reveals morphometric baculum differences for discriminating the cryptic species *Pipistrellus pipistrellus* and *P. pygmaeus*. *Acta Chiropterologica*, *16*(1), 157–168.

Herdina, A. N., Kelly, D. A., Jahelková, H., Lina, P. H. C., Horáček, I., & Metscher, B. D. (2015). Testing hypotheses of bat baculum function with 3D models derived from microCT. *Journal of Anatomy*, *226*(3), 229–235.

Hershkovitz, P. (1977). External genitalia and accessory structures. In P. Hershkovitz (Ed.), *Living New World monkeys (Platyrrhini) with an introduction to Primates* (Vol. 1(2), pp. 112–119). University of Chicago Press. Ch. 14.

Hershkovitz, P. (1993). *Male external genitalia of non-prehensile tailed South American monkeys*. Field Museum of Natural History.

Hill, O. W. C. (1966). Catarrhini, Cercopithecoidea, Cercopithecinae. In *Primates—Comparative Anatomy and Taxonomy* (p. 757). Edinburgh University Press. Ch. 6.

Hill, O. W. C. (1974). Cynopithecinae, Cercocebus, Macaca, Cynopithecus. In *Primates—Comparative Anatomy and Taxonomy* (p. 934). Edinburgh University Press. Ch. 7.

Hosken, D. J., & Stockley, P. (2004). Sexual selection and genital evolution. *Trends in Ecology & Evolution*, *19*(2), 87–93.

Huelsenbeck, J. P., Nielsen, R., & Bollback, J. P. (2003). Stochastic mapping of morphological characters. *Systematic Biology*, *52*(2), 131–158.

Kankilic, T., Kankilic, T., Şeker, P. S. O., & Kivanc, E. (2014). Morphological and biometricalcomparisons of the baculum in the genus *Nannospalax* Palmer, 1903 (Rodentia: Spalacidae) from Turkey with consideration of its taxonomic importance. *Turkish Journal of Zoology*, *38*(2), 144–157.

Kelly, D. A. (2000). Anatomy of the baculum–corpus cavernosum interface in the Norway rat (Rattus norvegicus), and implications for force transfer during copulation. *Journal of Morphology*, *244*(1), 69–77.

Klaczko, J., Ingram, T., & Losos, J. (2015). Genitals evolve faster than other traits in Anolis lizards. *Journal of Zoology*, *295*(1), 44–48.

Koenigswald, W. V. (1979). Ein lemurenrest aus dem eozänen Ölschiefer der Grube Messel bei Darmstadt. *Paläontologische Zeitschrift*, *53*, 63–76.

Koenigswald, W. V. (1985). Der dritte Lemurenrest aus dem mitteleozänen Olschiefer der Grube Messel bei Darmstadt. *Carolinea*, *42*, 145–148.

Larivière, S., & Ferguson, S. H. (2002). On the evolution of the mammalian baculum: vaginal friction, prolonged intromission or induced ovulation? *Mammal Review*, *32*(4), 283–294.

Leon-Alvarado, O. D., & Ramírez-Chaves, H. E. (2017). Morphological description of the glans penis and baculum of *Coendou quichua* (Rodentia: Erethizontidae). *Therya*, *8*(3), 263–268.

Long, C. A., & Frank, T. (1968). Morphometric variation and function in the baculum, with comments on correlation of parts. *Journal of Mammalogy*, *49*(1), 32–43.

Martin, R. D. (2007). The evolution of human reproduction: a primatological perspective. *American Journal of Physical Anthropology*, *134*(S45), 59–84.

Matthews, L. H. (1946). Notes on the genital anatomy and physiology of the gibbon (*Hylobates*). *Proceedings of the Zoological Society of London*, *116*(2), 339–364.

Nedyalkov, N., Vergilov, V., & Zlatkov, B. (2021). Penis morphology of two European mole species (Soricomorpha, Talpidae). *Biologia*, *76*(9), 2519–2525.

Nekaris, K. A. I. (2003). Observations of mating, birthing and parental behaviour in three subspecies of slender loris (*Loris tardigradus* and *Loris lydekkerianus*) in India and Sri Lanka. *Folia Primatologica*, *74*, 312–336.

Nielsen, R. (2002). Mapping mutations on phylogenies. *Systematic Biology*, *51*(5), 729–739.

Orr, T. J., & Brennan, P. L. (2016). All features great and small—the potential roles of the baculum and penile spines in mammals. *Integrative and Comparative Biology*, *56*(4), 635–643.

Pagel, M. (1999). Inferring the historical patterns of biological evolution. *Nature*, *401*(6756), 877–884.

Paradis, E., & Schliep, K. E. (2019). Ape 5.0: an environment for modern phylogenetics and evolutionary analyses in R. *Bioinformatics*, *35*(3), 526–528.

Patterson, B. D. (1983). Baculum-body size relationships as evidence for a selective continuum on bacular morphology. *Journal of Mammalogy*, *64*(3), 496–499.

Patterson, B. D., & Thaeler, J. C. S. (1982). The mammalian baculum: hypotheses on the nature of bacular variability. *Journal of Mammalogy*, *63*(1), 1–15.

Pocock, R. I. (1918). On the external characters of the lemurs and of Tarsius. *Journal of Zoology*, *88*(1–2), 19–53.

Pomidor, B. J., Makedonska, J., & Slice, D. E. (2016). A landmark-free method for three-dimensional shape analysis. *PLoS One*, *11*(3), e0150368.

Posada, D., & Buckley, T. R. (2004). Model selection and model averaging in phylogenetics: advantages of Akaike information

19328494, 0, Downloaded from https://anatomypubs.onlinelibrary.wiley.com/doi/10.1002/ar.70216 by CochraneItalia, Wiley Online Library on [04/05/2026]. See the Terms and Conditions (https://onlinelibrary.wiley.com/terms-and-conditions) on Wiley Online Library for rules of use; OA articles are governed by the applicable Creative Commons License

criterion and Bayesian approaches over likelihood ratio tests. *Systematic Biology*, *53*(5), 793–808.

Pozzi, L., Hodgson, J. A., Burrell, A. S., Sterner, K. N., Raaum, R. L., & Disotell, T. R. (2014). Primate phylogenetic relationships and divergence dates inferred from complete mitochondrial genomes. *Molecular Phylogenetics and Evolution*, *75*, 165–183.

Ramm, S. A. (2007). Sexual selection and genital evolution in mammals: a phylogenetic analysis of baculum length. *The American Naturalist*, *169*(3), 360–369.

Ramm, S. A., Khoo, L., & Stockley, P. (2010). Sexual selection and the rodent baculum: an intraspecific study in the house mouse (*Mus musculus domesticus*). *Genetica*, *138*(1), 129–137.

Ray, R. P., Nakata, T., Henningsson, P., & Bomphrey, R. J. (2016). Enhanced flight performance by genetic manipulation of wing shape in *Drosophila*. *Nature Communications*, *7*(1), 10851.

Revell, L. J. (2012). phytools: an R package for phylogenetic comparative biology (and other things). *Methods in Ecology and Evolution*, *3*(2), 217–223.

Revell, L. J. (2013). Two new graphical methods for mapping trait evolution on phylogenies. *Methods in Ecology and Evolution*, *4*(8), 754–759.

Rohlf, F. J., & Slice, D. (1990). Extensions of the Procrustes method for the optimal superimposition of landmarks. *Systematic Biology*, *39*(1), 40–59.

Romer, A. S., & Parsons, T. S. (1996). *Anatomia comparata dei vertebrati* (p. 736). Edises.

Scalici, M., Spani, F., Traversetti, L., Carpaneto, G. M., & Piras, P. (2018). Cranial shape parallelism in soft-furred sengis: moving on a geographic gradient. *Journal of Mammalogy*, *99*(6), 1375–1386.

Schultz, N. G., Lough-Stevens, M., Abreu, E., Orr, T., & Dean, M. D. (2016). The baculum was gained and lost multiple times during mammalian evolution. *Integrative and Comparative Biology*, *56*(4), 644–656.

Shan, S., Kovalsky, S. Z., Winchester, J. M., Boyer, D. M., & Daubechies, I. (2019). ariaDNE: A robustly implemented algorithm for Dirichlet energy of the normal. *Methods in Ecology and Evolution*, *10*, 541–552.

Shao, Y., Zhou, L., Li, F., Zhao, L., Zhang, B. L., Shao, F., Chen, J. W., Chen, C. Y., Bi, X., Zhuang, X. L., Zhu, H. L., Hu, J., Sun, Z., Li, X., Wang, D., Rivas-González, I., Wang, S., Wang, Y. M., Chen, W., … Wu, D. D. (2023). Phylogenomic analyses provide insights into primate evolution. *Science*, *380*(6648), 913–924.

Simmons, L. W. (2014). Sexual selection and genital evolution. *Austral Entomology*, *53*(1), 1–17.

Simmons, L. W., & Firman, R. C. (2014). Experimental evidence for the evolution of the mammalian baculum by sexual selection. *Evolution*, *68*(1), 276–283.

Spani, F., Morigi, M. P., Bettuzzi, M., Scalici, M., & Carosi, M. (2020). A 3D journey on virtual surfaces and inner structure of ossa genitalia in primates by means of a non-invasive imaging tool. *PLoS One*, *15*(1), e0228131.

Spani, F., Morigi, M. P., Bettuzzi, M., Scalici, M., Gentile, G., & Carosi, M. (2021). The ultimate database to (re) set the evolutionary history of primate genital bones. *Scientific Reports*, *11*, 1–15.

Spani, F., Morigi, M. P., Bettuzzi, M., Scalici, M., Gentile, G., & Carosi, M. (2022). Over and beyond the primate *baubellum* surface: A "Jewel Bone" shielded in museums. *Applied Sciences*, *12*(4), 2096.

Spani, F., Scalici, M., Crandall, K. A., & Piras, P. (2020). Claw asymmetry in crabs: approaching an old issue from a new point of view. *Biological Journal of the Linnean Society*, *129*(1), 162–176.

Stockley, P. (2012). The baculum. *Current Biology*, *22*(24), R1032–R1033.

Stockley, P., Ramm, S. A., Sherborne, A. L., Thom, M. D., Paterson, S., & Hurst, J. L. (2013). Baculum morphology predicts reproductive success of male house mice under sexual selection. *BMC Biology*, *11*(1), 66.

Tardif, S., Carville, A., Elmore, D., Williams, L. E., & Rice, K. (2012). Reproduction and breeding of nonhuman primates. In C. R. Abee, K. Mansfield, S. Tardif, & T. Morris (Eds.), *Nonhuman primates in biomedical research* (pp. 197–249). Academic Press.

Tumlison, R., & McDaniel, V. R. (1984). A description of the baculum of the bobcat (*Felis rufus*), with comments on its development and taxonomic implications. *Canadian Journal of Zoology*, *62*(6), 1172–1176.

Uhlenbeck, G. E., & Ornstein, L. S. (1930). On the theory of Brownian motion. *Physical Review*, *36*, 823–841.

Weimann, B., Edwards, M. A., & Jass, C. N. (2014). Identification of the baculum in American pika (*Ochotona princeps*: lagomorpha) from southwestern Alberta, Canada. *Journal of Mammalogy*, *95*(2), 284–289.

Wiener, N. (1923). Differential space. *Journal of Mathematical Physics*, *2*, 131–174.

SUPPORTING INFORMATION

Additional supporting information can be found online in the Supporting Information section at the end of this article.

How to cite this article: Spani, F., Morigi, M. P., Bettuzzi, M., & Carosi, M. (2026). Tracing the evolutionary history of the morpho-anatomy of baculum in primates. *The Anatomical Record*, 1–17. https://doi.org/10.1002/ar.70216

19328494, 0, Downloaded from https://anatomypubs.onlinelibrary.wiley.com/doi/10.1002/ar.70216 by CochraneItalia, Wiley Online Library on [04/05/2026]. See the Terms and Conditions (https://onlinelibrary.wiley.com/terms-and-conditions) on Wiley Online Library for rules of use; OA articles are governed by the applicable Creative Commons License